

# Synchronization Defects and Broken Symmetry in Spiral Waves

Andrei Goryachev<sup>1</sup>, Hugues Chaté<sup>2</sup>, and Raymond Kapral<sup>1</sup>

<sup>1</sup>*Chemical Physics Theory Group, Department of Chemistry, University of Toronto, Toronto, ON M5S 3H6, Canada*

<sup>2</sup>*CEA — Service de Physique de l'Etat Condensé, Centre d'Etudes de Saclay, 91191 Gif-sur-Yvette, France*

Spiral waves are investigated in oscillatory media exhibiting period-doubling bifurcations. In the period-doubled and chaotic regimes, the rotational symmetry of the spiral wave is broken. The loss of symmetry takes the form of synchronization defect lines where the phase of the local oscillation changes by multiples of  $2\pi$ . The internal structure and geometry of these synchronization defects is studied and a discussion of the possible types of defect lines is presented.

82.20.Wt, 05.40.+j, 05.60.+w, 51.10.+y

Spatially-distributed oscillatory media may undergo bifurcations where the period of the orbit doubles at almost every point in the system. In the simple oscillatory regime (period-1), before such period-doubling bifurcations occur, the system may support stable rotationally-symmetric spiral wave solutions. [1] The dynamics in this regime is typically described by the complex Ginzburg-Landau (CGL) equation, the generic equation for an oscillatory medium near the Hopf bifurcation point at which oscillations appear [2]. Spiral waves are a well-known feature of this regime where they have been intensively studied [3]. However, they can also exist in media where the local dynamics is complex-periodic or chaotic [4–6]. In this Letter, we investigate the consequences of period-doubling bifurcations on the structure and dynamics of spiral waves. We find that the symmetry of the spiral wave is broken by defect lines where the phase of the oscillation changes by multiples of  $2\pi$ , and we study the nature of these synchronization defect lines.

We consider the dynamics of spatially-distributed systems governed by reaction-diffusion equations of the form

$$\frac{\partial \mathbf{c}(\mathbf{r}, t)}{\partial t} = \mathbf{R}(\mathbf{c}(\mathbf{r}, t)) + D\nabla^2 \mathbf{c}(\mathbf{r}, t), \quad (1)$$

where  $\mathbf{c}(\mathbf{r}, t)$  is a vector of local concentrations,  $D$  is the diffusion coefficient and  $\mathbf{R}(\mathbf{c}(\mathbf{r}, t))$  describes the local reaction kinetics. While the phenomena we investigate should be observable for any spatially-distributed system exhibiting period-doubling, we have considered cases where the spatially-homogeneous system  $\dot{\mathbf{c}}(t) = \mathbf{R}(\mathbf{c}(t))$  itself exhibits period-doubling bifurcations. Specifically, the calculations described here were carried out on the Rössler model,  $R_x = -c_y - c_z$ ,  $R_y = c_x + Ac_y$ ,  $R_z = c_x c_z - Cc_z + B$ , which is well known to exhibit chaos arising from a cascade of subharmonic bifurcations.

Spiral waves were initiated as in [5,6], taking advantage of the cyclic character of the projection of the Rössler attractor on the  $(c_x, c_y)$  plane. Various values of the parameter  $C$  in the interval  $[2.5, 6.0]$  were considered, while the other parameters were fixed at  $A = 0.2$  and  $B = 0.2$ . The scaled diffusion coefficient was  $D\Delta t/(\Delta r)^2 = 1.6 \times 10^{-2}$  ( $\Delta t = 10^{-2}$ ) in all calculations. Simulations were carried out on a disk-shaped domain of radius 255 with no-flux boundary conditions. In the period-1 regime, the

medium supports a single, stable, one-armed spiral wave. As the parameter  $C$  increases, the local dynamics undergoes a period-doubling bifurcation at  $C = C^* \approx 3.03$ . (The spatially-homogeneous Rössler model bifurcates at  $C_{\text{ode}}^* \approx 2.83$ ). In order to quantitatively characterize this transition, it is convenient to introduce a local order parameter  $\delta c_z(\mathbf{r})$ , defined as the difference between two successive maxima of the time series  $c_z(\mathbf{r}, t)$ .

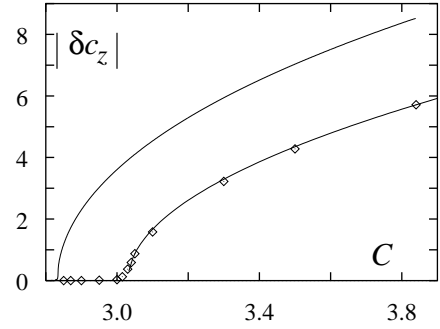


FIG. 1. Bifurcation diagram, constructed at  $r_0 = 130$ , showing the first period-doubling bifurcation in the medium supporting a single spiral wave (diamonds). For comparison, the upper left curve is the bifurcation diagram for a spatially homogeneous system.

Figure 1 shows the dependence of  $\delta c_z(r_0)$  on  $C$  calculated at a typical point at radius  $r_0 = 130$ , sufficiently far from both the boundary and the core of the spiral. One observes a parabolic increase in  $\delta c_z(r_0)$  beyond  $C^* \approx 3.03$ , typical of a supercritical period-doubling bifurcation. This behavior is seen at almost every point in the medium (the structure is difficult to resolve deep in the core region). Along almost any ray emanating from the core, the magnitude of  $\delta c_z(r)$  varies as  $A(r)\sqrt{C - C^*}$  where  $A(r)$  behaves like the amplitude profile of the spiral itself, i.e.,  $A(r) \simeq r^\alpha$  in the core region and is constant elsewhere except near the boundary.

Within the period-2 domain, the spiral wave acquires a global structure different from that in a simple periodic medium. Figure 2 shows the  $c_z(\mathbf{r}, t_0)$  concentration field at a single time instant  $t_0$ . The alternation of high and low  $c_z(\mathbf{r}, t_0)$  maxima unambiguously demonstrates

that period-2 local temporal dynamics manifests itself in the formation of a period-doubled spiral waveform with broken rotational symmetry whose wavelength is twice that of the original spiral wave in the period-1 medium. The lower panel of Fig. 2 shows  $c_z(\mathbf{r}, t_0)$  in grey shades and indicates the curve connecting the spiral core and the boundary, denoted as  $\Omega$ , where sharp changes in the concentration occur. The  $\Omega$  curve plays a central role in the organization of the spiral wave, and its character will be examined below.



FIG. 2. Spiral wave in a medium with period-2 local dynamics at  $C = 3.84$ . Concentration field  $c_z(\mathbf{r}, t_0)$  is shown as elevation in the upper panel and as grey shades in the lower panel. The solid line depicts the  $\Omega$  curve. The arc segment at radius  $r_0 = 130$  along which points were taken to construct Figs. 3-5 is also shown.

The fact that the local dynamics is almost everywhere period-2 endows the spiral with some unusual features: unlike a period-1 medium where the concentration is periodic with the period of the spiral rotation, here, after one turn of the spiral, the high and low maxima interchange and it is only after two spiral periods that the concentration field is restored to its initial value. Although the spiral rotates, the  $\Omega$  curve is, up to numerical accuracy, stationary. In the asymptotic regime, after transients depending on the initial condition, the shape of the  $\Omega$  curve takes the form of a straight line segment

with a short curved portion lying inside the core region. Figure 3 shows  $\delta c_z(\theta)$  for three values of  $C$  as function of the polar angle  $\theta$  along the arc segment that crosses the  $\Omega$  curve. To a very good approximation, the numerical data show that  $\delta c_z(r, \theta, C)$  varies like

$$\delta c_z(r, \theta, C) \simeq A(r)\sqrt{C-C^*} \tanh[\kappa r(\theta-\theta_\Omega)(C-C^*)] \quad (2)$$

where  $\theta_\Omega$  is the angular position of the  $\Omega$  curve and  $\kappa$  is a numerical factor. The  $\Omega$  curve is thus a localized object whose width remains approximately constant with  $r$  and varies like  $1/(C-C^*)$ . As  $C$  approaches  $C^*$  from above, the width increases until it becomes comparable to  $2\pi$  and the  $\Omega$  curve ceases to be a well-defined object [7].

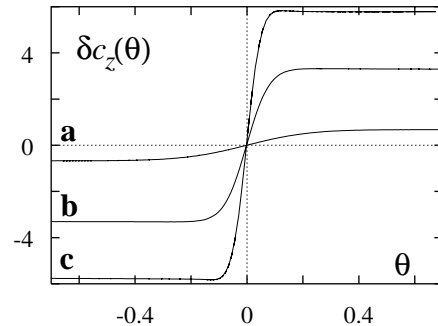


FIG. 3. Order parameter  $\delta c_z(\theta)$  profile across the  $\Omega$  curve along the arc at radius  $r_0 = 130$  indicated in the lower panel of Fig. 2 for three values of  $C$ : (a)  $C = 3.04$ , (b)  $C = 3.10$ , (c)  $C = 3.84$ . Curve (c) is calculated for the medium in Fig. 2.

We now show that the  $\Omega$  curve corresponds to a one-dimensional synchronization defect across which the phase of oscillation changes by some multiple of  $2\pi$ . One can always uniquely parametrize an orbit of a period-1 oscillation by a phase variable  $\varphi \in [0, 2\pi)$  and describe the spatially-distributed medium by a phase field  $\varphi(\mathbf{r}, t)$ . At the center of the spiral lies a point defect of this field characterized by a topological charge  $\frac{1}{2\pi} \oint \nabla \varphi(\mathbf{r}, t) \cdot d\mathbf{l} = n_t$  [8], where the integral is taken along a closed curve encircling the defect. There exist several possible ways to extend the definition of phase for complex-periodic oscillations [9]. We assume that the phase  $\phi(t)$  of an  $n$ -periodic oscillation is a scalar function of time which increases monotonically by  $2\pi n$  for each full period of the oscillation  $T_n$ . For some systems,  $\phi$  can be defined in terms of an angle variable in a suitably-chosen coordinate frame in phase space. For the Rössler model we use a cylindrical coordinate system  $(\rho, \varphi, z)$  with origin at the unstable fixed point of the spatially-homogenous system and  $z$  along  $c_z$ . The phase variable  $\phi \in [0, 2\pi n)$  then takes the form  $\phi = \varphi + 2\pi m$  where  $m$  is an integer with values from 0 to  $n-1$ . While  $\varphi$  is a single-valued function of the original dynamical variables, the phase  $\phi$  of a complex-periodic oscillation is not an observable, since a knowledge of the entire local orbit is required in order to calculate  $m$ .

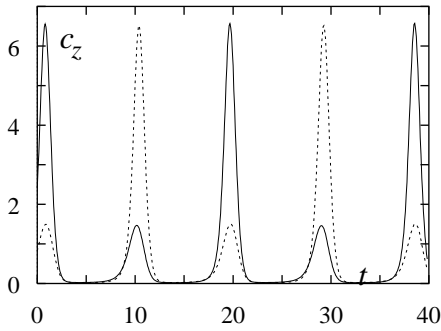


FIG. 4. Two  $c_z(t)$  concentration time series calculated for the medium shown in Fig. 2 at points  $\mathbf{r}_{1,3} = (r_0 = 130, \theta_\Omega \pm 0.05)$  on opposite sides of the  $\Omega$  curve.

The  $\Omega$  curve can be viewed as a one-dimensional defect of the  $\phi(\mathbf{r}, t)$  field. Figure 4 shows two  $c_z(t)$  concentration time series at nearby spatial points on either side of the  $\Omega$  curve. The two oscillations are shifted relative to each other by half a period. For a period-2 oscillation, this corresponds to a phase shift of  $\delta\phi = 2\pi$ . The necessity for such a phase synchronization slip in a one-armed spiral in a period-doubled medium can be understood from the following argument. Consider a contour integral of the phase gradient  $\nabla\phi(\mathbf{r}, t)$  taken along a closed loop  $\Gamma$  which surrounds the core of the spiral wave. For an arbitrary point  $\mathbf{r}_0 \in \Gamma$ , this loop is just a path in the medium which starts at  $\mathbf{r}_0$ , described by the local  $n$ -periodic oscillation phase  $\phi(\mathbf{r}, t)$ , and returns to the same point with same oscillation phase  $\phi(\mathbf{r}, t)$ . Thus, the integral may take only values  $2\pi nk$  equal to multiples of the full-period phase increment. Since the phase field is given by  $\phi(\mathbf{r}, t) = \varphi(\mathbf{r}, t) + 2\pi m(\mathbf{r}, t)$ , we find

$$\oint \nabla\phi(\mathbf{r}, t) \cdot d\mathbf{l} = \oint \nabla\varphi(\mathbf{r}, t) \cdot d\mathbf{l} + 2\pi \oint \nabla m(\mathbf{r}, t) \cdot d\mathbf{l}. \quad (3)$$

Simulations for a one-armed spiral show that, at any given time  $t$ ,  $\oint \nabla\varphi(\mathbf{r}, t) \cdot d\mathbf{l} = \pm 2\pi$ , regardless of the periodicity of the local dynamics [10]. Given that the full-period phase increment is  $2\pi$  only in the case of period-1 dynamics with  $m(\mathbf{r}, t) \equiv 0$ , for period-doubled dynamics the integration of  $\nabla m(\mathbf{r}, t)$  along  $\Gamma$  must yield a non-zero contribution to balance (3). Since  $m(\mathbf{r}, t)$  is an integer function, its value changes discontinuously with time and space so that  $\nabla m(\mathbf{r}, t)$  is different from zero only at a single point: the intersection of  $\Gamma$  with the  $\Omega$  curve. For a period-2 medium, the addition of a  $2\pi$  phase jump on the  $\Omega$  curve and a  $2\pi$  contribution from integration of  $\varphi(\mathbf{r}, t)$  yields the necessary full-period increment of  $4\pi$ .

The nature of the phase jump associated with the  $\Omega$  curve can be understood from the observation of the local orbit loop exchange which occurs on the scale of the  $\Omega$  curve width. Figure 5 shows local orbits calculated at  $r_0 = 130$  for three angles  $\theta_1 = \theta_\Omega - 0.05, \theta_2 = \theta_\Omega, \theta_3 = \theta_\Omega + 0.05$ . (The corresponding  $c_z(t)$  time series for the first and last orbits are shown in Fig. 4 and  $\delta c_z(\theta)$  is given in Fig. 3(c).) Consider local orbits on the arc connecting points  $\theta_1$  and  $\theta_3$  (cf. Fig. 2). As one traverses the

arc, the larger, outer loop of the local orbit constantly shrinks while the smaller, inner loop grows. At  $\theta = \theta_\Omega$ , both loops merge and then pass each other exchanging their positions in phase space. (Compare Figs. 5(a) and (c).) The behavior of the  $\delta c_z(\theta)$  order parameter along the arc provides only limited information on the loop exchange. As one sees from Fig. 5, not only are the  $c_z$  maximum values of two loops equal ( $\delta c_z(\theta_\Omega) = 0$ ), but the entire loops coincide in phase space: at the exchange point  $\theta = \theta_\Omega$ , the local oscillation is effectively period-1 [6]. Continuity of the medium requires that the period-1 points form a line extending from the core to the boundary: the  $\Omega$  curve.

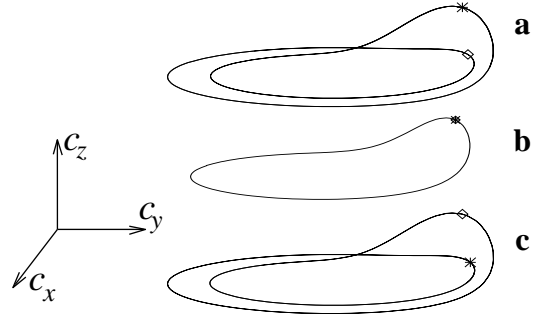


FIG. 5. Loop exchange in local orbits as the  $\Omega$  curve is crossed (see text). Data collected on the arc shown in Fig. 2: (a)  $\theta_1 = \theta_\Omega - 0.05$ ; (b)  $\theta_2 = \theta_\Omega$ ; (c)  $\theta_3 = \theta_\Omega + 0.05$ . Two points corresponding to time instants  $t_1 = 10.3$  (diamond) and  $t_2 = 19.8$  (asterisk) are marked on each trajectory to highlight the exchange.

The  $\Omega$  curve separates domains that are dynamically equivalent apart from a phase shift and it should have no net velocity in its normal direction. Outside the core region, where the  $\Omega$  curve width is small on the scale of the spiral wavelength, any large-scale curvature will be eliminated by motion of the  $\Omega$  curve. This motion, induced by the mean curvature and proportional to the diffusion coefficient, will yield a straight  $\Omega$  curve. In the core region, the  $\Omega$  curve width is comparable to the length scale of other concentration gradients and more complicated structure is possible. [6]

We now consider more complex local oscillations. At  $C \approx 4.09$ , the system undergoes a bifurcation to period 4 which can be described by an order parameter  $\delta_2 c_z(\mathbf{r})$ , analogous to  $\delta c_z(\mathbf{r})$ , defined as the difference between the first and third or second and fourth  $c_z(\mathbf{r}, t)$  maxima within one full period of the oscillation. This can be generalized to any period- $2^k$  regime. An oscillatory medium with period-4 local dynamics has two types of synchronization defect lines:  $\Omega_1$  and  $\Omega_2$  curves with associated phase jump values of  $\pm 6\pi$  and  $4\pi$ , respectively [11]. These curves are shown in Fig. 6 for  $C = 4.3$ .

We may number the loops of the local period-4 cycles successively according to their positions in phase space starting from the innermost loop. Then the  $\Omega_1$  curve

corresponds to the  $(\begin{smallmatrix} 1234 \\ 4312 \end{smallmatrix})$  loop exchange altering all four loops, while the  $\Omega_2$  curve is attributed to the  $(\begin{smallmatrix} 1234 \\ 2143 \end{smallmatrix})$  exchange which involves only rearrangement of loops inside the period-2 bands. By considering topological braid properties of a period-doubled orbit [6], all possible loop exchanges can be enumerated. Outside the core region, we expect that there exist  $k$  types of  $\Omega$  curves in a period- $2^k$  medium.



FIG. 6. Synchronization domains delimited by  $\Omega_1$  and  $\Omega_2$  curves in a medium with period-4 dynamics. The maximum value of  $c_z(\mathbf{r})$  in one spiral rotation is plotted as grey shades. Apart from boundary effects, roughly four levels are observed, corresponding to the four loops of the local orbit, from loop 1 (darkest shade) to loop 4 (lightest shade).

The argument given above for the value of the  $\oint \nabla\phi(\mathbf{r}, t) \cdot d\mathbf{l}$  integral applies to a period-4 medium as well. The existence of two types of defect provides several ways to satisfy condition (3). Thus, a medium with a one-armed spiral wave characterized by  $n_t = +1$  may have one  $\Omega_1$  curve with  $+6\pi$  phase shift or both  $\Omega_1$  ( $-6\pi$ ) and  $\Omega_2$  ( $4\pi$ ) curves. Configurations where more than two curves originate in the same spiral core are, in principle, possible. However, they were not observed starting from the initial conditions considered here.

For higher values of  $C$ , the  $\Omega$  curves may evolve in time leading to spatio-temporal chaotic regimes within the general spiral structure. The curves separate domains of near synchronization where the local phase  $\phi(\mathbf{r}, t)$  changes continuously but experiences sudden jumps when a domain boundary is crossed. A full exploration of the dynamics of  $\Omega$  curves in this and other parameter regimes remains to be carried out.

Wavelength-doubled spiral waves have been observed in recent experiments on the Belousov-Zhabotinsky (BZ) reaction in ruthenium-complex monolayers on the surface of a BZ solution. [12] The experimentally observed spiral wave structure with a clearly visible  $\Omega$  curve (cf. Fig. 5 of Ref. [12]) is identical to that in Fig. 2. Not only is the final wavelength-doubled spiral wave structure the same,

but the dynamics leading to its formation from an initial period-1 spiral is also the same as that observed in the experiment. We have demonstrated that such broken-symmetry spiral waves are necessarily formed when the local dynamics has period-2 character, as is the case in Ref. [12]. Although our results were obtained for a system possessing a period-doubling cascade, we believe that the synchronization defect lines are generic features of distributed media exhibiting complex periodic behavior, independent of the specific origin of this periodicity. Thus, we expect the phenomena described in this Letter to be observable in excitable as well as oscillatory media where such period- $n$  local dynamics is observed.

Work supported in part by a grant from the Natural Sciences and Engineering Research Council of Canada. We would like to thank M. Golubitsky for discussions on symmetry breaking and period-doubling bifurcations.

- 
- [1] See, for example, V. Petrov, Q. Ouyang and H. L. Swinney, *Nature*, **388**, 655 (1997).
  - [2] Y. Kuramoto, *Chemical Oscillations, Waves, and Turbulence*, (Springer-Verlag, Berlin, 1984).
  - [3] See, e.g., I. S. Aranson, L. Kramer and A. Weber, *Phys. Rev. E* **47**, 3231 (1993).
  - [4] R. Klevecz, J. Pilliod and J. Bolen, *Chronobiology International* **8**, 6 (1991).
  - [5] L. Brunnet, H. Chaté and P. Manneville, *Physica D* **78**, 141 (1994).
  - [6] A. Goryachev and R. Kapral, *Phys. Rev. Lett.* **76**, 1619 (1996); A. Goryachev and R. Kapral, *Phys. Rev. E* **54**, 5469 (1996).
  - [7] The localized character of the  $\Omega$  curve can be understood intuitively as a consequence of the existence of the unstable orbit separating the two loops of the cycle in the local phase space. In this respect, the curve is similar to a kink in a bistable system.
  - [8] N.D. Mermin, *Rev. Mod. Phys.* **51**, 591 (1979).
  - [9] M. Rosenblum, A. Pikovsky and J. Kurths, *Phys. Rev. Lett.* **76**, 1804 (1996); G. Osipov, A. Pikovsky, M. Rosenblum and J. Kurths, *Phys. Rev. E* **55**, 2353 (1997).
  - [10] Initial conditions corresponding to the full  $4\pi$  period-2 cycle led to a bound state of two single-armed spirals, much as in the CGL equation [3], where spirals with a topological charge  $|n_t| > 1$  are unstable, see: P.S. Hagan, *SIAM J. Appl. Math.* **42**, 762 (1982).
  - [11] The phase shift for the  $\Omega_2$  curve is  $4\pi$ , i.e., exactly equal to one half of a full-period phase increment of  $8\pi$ . Thus, it is impossible to distinguish oscillations shifted forward or backward by  $4\pi$ , and the phase shift of the  $\Omega_2$  curve is left unsigned, like that for the  $\Omega$  curve for period-2.
  - [12] M. Yoneyama, A. Fujii and S. Maeda, *J. Am. Chem. Soc.* **117**, 8188 (1995).